SAE Technical Paper Series

FREEDOM THROUGH MOBILITY S·A·E 1905·1980 75th anniversary

790407

# Material and Processing Effects on Fatigue Performance of Leaf Springs

R. W. Landgraf and R. C. Francis
Ford Motor Co.

Congress and Exposition
Cobo Hall, Detroit
February 26-March 2, 1979

SOCIETY OF AUTOMOTIVE ENGINEERS, INC.
400 COMMONWEALTH DRIVE
WARRENDALE, PENNSYLVANIA 15096

**ISSN 0148-7191**

# Material and Processing Effects on Fatigue Performance of Leaf Springs

**R. W. Landgraf and R. C. Francis**
Ford Motor Co.

THE MECHANICAL PERFORMANCE of vehicle leaf springs is influenced, in a complex way, by a number of material and processing details. For example, in the course of manufacture, spring steel is typically subjected to hot forming and heat treating operations followed by mechanical processing such as shot peening and presetting. Each of these steps can significantly affect the structure and properties of the material as well as the residual stress patterns built up in surface layers [1,2)*. From a design standpoint, it is important to have methods available to predict how various processing sequences will influence fatigue behavior so that designs can be optimized. Spring performance will depend on material properties, as influenced by processing, the magnitude and stability of residual stresses, and service loading environment. Fatigue analysis procedures are now available for combining such information for the purpose of making life predictions [3).

In Fig. 1 are listed the various spring design considerations. Forming and heat treatment operations will affect material hardness, both through heat treat response and surface decarburization. Mechanical processing will affect residual stress patterns and spring geometry. Finally service loading may alter original residual stress levels as a result of cyclic stress relaxation. In this paper, the material behavior characteristics related to spring performance are first determined. The effect of component processing on these characteristics is then documented followed by a demonstration of the application of these concepts to component fatigue life prediction.

## EXPERIMENTAL PROGRAM

Axial and bending specimens of SAE 5160 spring steel, of the designs shown in Fig. 2, were prepared and heat treated to three different hardness levels: 407, 440 and 460 HB. Axial tests, performed in a closed-loop, servo-hydraulic test system, were used

*Numbers in parentheses designate References at end of paper.

## ABSTRACT

Procedures are developed for assessing the influence of various material and processing factors on the fatigue performance of leaf springs. Cyclic material properties, determined from smooth axial specimens of spring steel, are used to determine the level and cyclic stability of residual stresses resulting from mechanical processing as well as the amount of permanent deformation associated with presetting operations. A damage parameter, incorporating material properties, residual stress effects and applied stressing conditions, is used to predict failure location, i.e. surface or subsurface, and lifetime as a function of processing sequence. Predictions are found to be in good agreement with experimental bending results.

0148-7191/79/0226-0407$02.50

## SPRING DESIGN CONSIDERATIONS

| Processing: | Effects |
|---|---|
| Hot forming | Hardness |
| Heat treatment | Decarb. |
| Shot peening | Resid. stress |
| Strain peening | |
| Presetting | Perman. set |
| Service Loading | Stress relax. |

Fig. 1 - The effects of processing variables and service loading on leaf springs

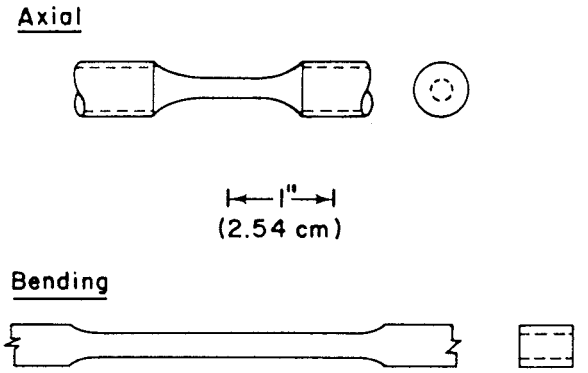


Fig. 2 - Axial and bending specimen configurations used in experimental program

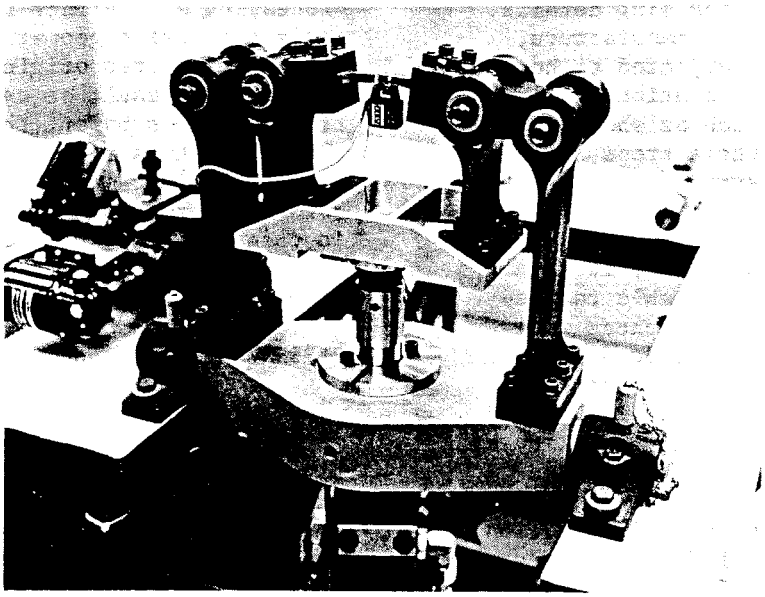

Fig. 3 - Four-point bending apparatus installed on servo-hydraulic actuator

to develop properties characterizing the cyclic deformation and fracture behavior of the steel (4) and to simulate patterns of behavior, e.g. stress relaxation, known to occur in springs. Bending specimens were subjected to various spring precessing sequences, such as shot peening, strain peening and presetting, followed by fatigue testing in the fixture shown in Fig. 3. This was an attempt to simulate leaf spring performance in a controlled and economical way. Residual stress profiles were determined from X-ray diffraction measurements.

### MATERIAL BEHAVIOR CONSIDERATIONS

Of particular concern in fatigue problems is the tendency for material properties to change as a result of cyclic deformation. This circumstance requires the determination of a cyclic stress-strain relation (5) for fatigue analysis. The monotonic and cyclic stress-

strain behavior of the 5160 steel is shown in Fig. 4. As a result of cyclic softening, the flow properties are seen to be reduced to about two-thirds of their original values. Such stress-strain curves are conveniently characterized by a power-law relation between stress and plastic strain:

$$\sigma = K\,(\varepsilon_p)^n \qquad (1)$$

Such a formulation will later be used to analyze mechanical prestressing effects. (See nomenclature list for definition of symbols.)

The constant amplitude fatigue resistance of 5160 steel is shown in Fig. 5 in the form of a strain amplitude-reversals to failure plot. The scatter-band in the figure indicates the 95% confidence interval for the test data. Strain cycling resistance is viewed as the summation of elastic and plastic strain resistance yielding a relation of the following form (6):

$$\frac{\Delta\varepsilon}{2} = \frac{\sigma'_f}{E}\,(2N_f)^b + \varepsilon'_f\,(2N_f)^c \qquad (2)$$

Mean stress effects can be included in Equation 2 as follows:

$$\frac{\Delta\varepsilon}{2} = \frac{\sigma'_f - \sigma_o}{E}\,(2N_f)^b + \varepsilon'_f\,(2N_f)^c \qquad (3)$$

where $\sigma_o$ = mean stress.
At long lives, greater than $10^5$, where behavior is nominally elastic, this can be simplified to the following stress-based form:

$$\frac{\sigma_a}{(\sigma'_f - \sigma_o)} = (2N_f)^b \qquad (4)$$

where $\sigma_a$ = applied stress amplitude.
In Fig. 6 is shown a material characterization sheet tabulating processing and properties for the 440 HB condition.

When considering the effect of residual stresses on fatigue, it is important to consider conditions under which they will be stable, i.e. cyclic stress relaxation may negate their effect (7). Such behavior is shown in Fig. 7 for a heat treated steel subjected to alternate zero-max., zero-min. cycling. Under such straining, the load (stress) response is observed to relax towards a completely reversed configuration, an indication of mean (residual) stress relaxation. By performing such tests at different strain amplitudes, it is possible to generate relaxation curves as shown in Fig. 8. This behavior can be described by the following relation:

$$\sigma_{oN} = \sigma_{o1}\,(N)^r \qquad (5)$$

where $\sigma_{oN}$ = mean (residual) stress, Nth cycle
$\sigma_{o1}$ = mean (residual) stress, 1st cycle
$r \equiv$ relaxation exponent, dependent upon hardness and strain amplitude.

By extrapolating such information to a zero relaxation rate, a threshold strain amplitude, below which relaxation will not occur, can be

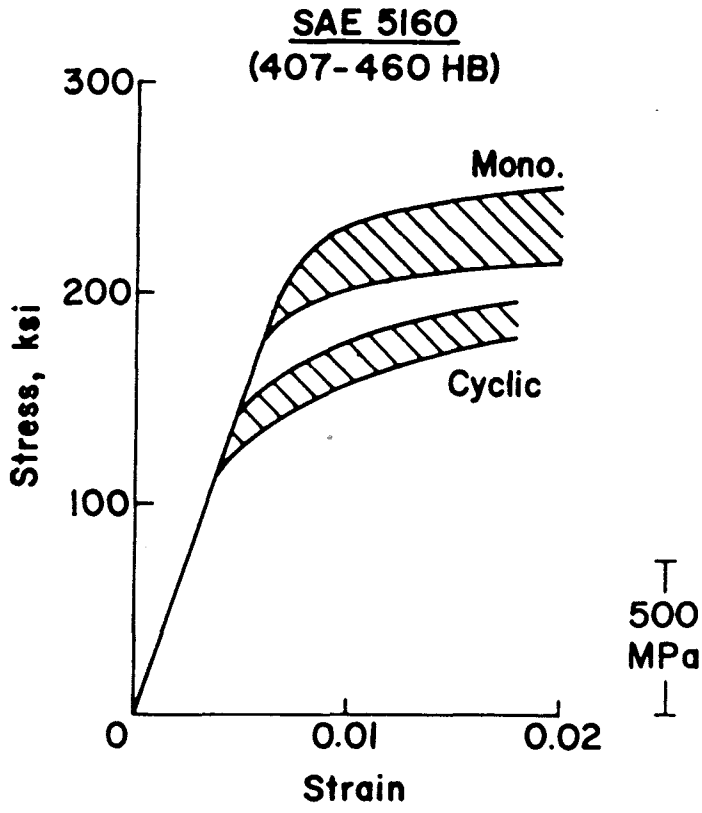


Fig. 4 - Monotonic and cyclic stress-strain curves for SAE 5160 spring steel

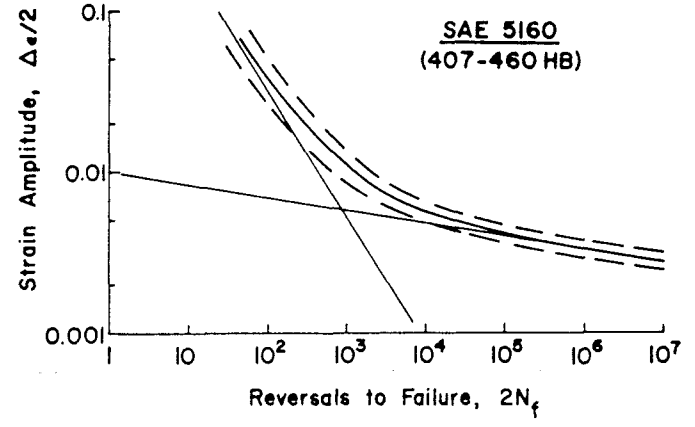


Fig. 5 - Strain-life curve for SAE 5160 spring steel. Dashed band indicates 95% confidence interval

Material SAE 5160

Condition Quenched & Tempered

Hardness 440 HB Other Specs.

Material Source Vendor

Specimen Orientation Longitudinal

Composition 0.61C, 0.86Mn, 0.02P, 0.02S, 0.31Si, 0.78Cr

Reference B. T. Crandall Date 3/77

Microstructure:

Grain Size

Tempered martensite

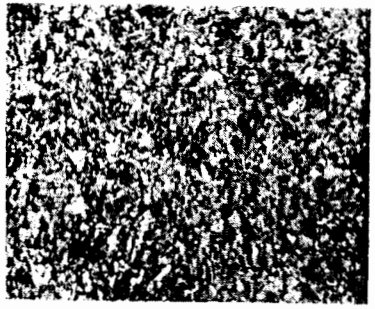


Comments:

Austenitized: 1650°F/30 min.
Agitated oil quench
Tempered: 825°F/1 hr.

Monotonic Properties:

| | | | | |
|---|---|---|---|---|
| Mod. of Elast., E | 205 | GPa ( | 29.5 | x 10³ ksi) |
| Yield Strength, 0.2% $S_y$ | 1450 | MPa ( | 210 | ksi) |
| Ultimate Strength, $S_u$ | 1550 | MPa ( | 225 | ksi) |
| Strength Coeff., K | 1895 | MPa ( | 275 | ksi) |
| Strain Hard. Exp., n | 0.046 | | | |
| Red. in Area, % RA | 43 | | | |
| True Frac. Strength, $\sigma_f$ | 1930 | MPa ( | 280 | ksi) |
| True Frac. Ductility, $\epsilon_f$ | 0.56 | | | |

Cyclic Properties:

| | | | | Correlation Coeff., r |
|---|---|---|---|---|
| Yield Strength, 0.2% $S_y'$ | 1070 | MPa ( | 155 | ksi) |
| Strength Coeff., K' | 2000 | MPa ( | 290 | ksi) |
| Strain Hard. Exp., n' | 0.10 | | | 0.92 |
| Fatigue Strength Coeff., $\sigma_f'$ | 2050 | MPa ( | 297 | ksi) |
| Fatigue Strength Exp., b | -0.09 | | | -0.94 |
| Fatigue Ductility Coeff., $\epsilon_f'$ | 1.24 | | | |
| Fatigue Ductility Exp., c | -0.79 | | | -0.95 |

Fig. 6 - Material characterization sheet for SAE 5160 spring steel

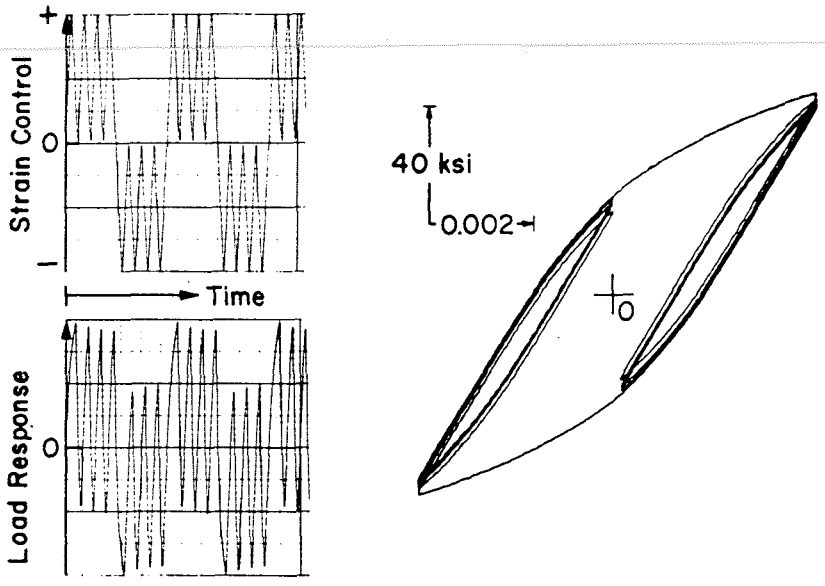


Fig. 7 - Example of cycle-dependent mean stress relaxation

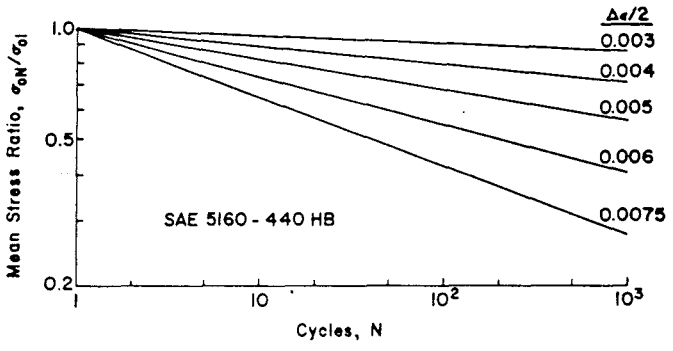


Fig. 8 - Representation of mean stress relaxation rates for various strain amplitudes

defined. For 5160 steel at 440HB, this threshold is 0.0024, or a stress amplitude of 70 ksi (483 MPa).

The cyclic properties and parameters developed in this section will next be applied to the analysis and interpretation of processing effects.

PROCESSING EFFECTS

HEAT TREATMENT - Heat treating effects, including decarburization, are conveniently interpreted in terms of material hardness. The fatigue property most affected by hardness variation is the fatigue strength coefficient, $\sigma'_f$. If this property is known at a particular hardness, $HB_o$, the value at any other hardness, HB, can be determined from:

$$\sigma'_f = \sigma'_{f_o} + 0.57\ (HB - HB_o) \qquad (6)$$

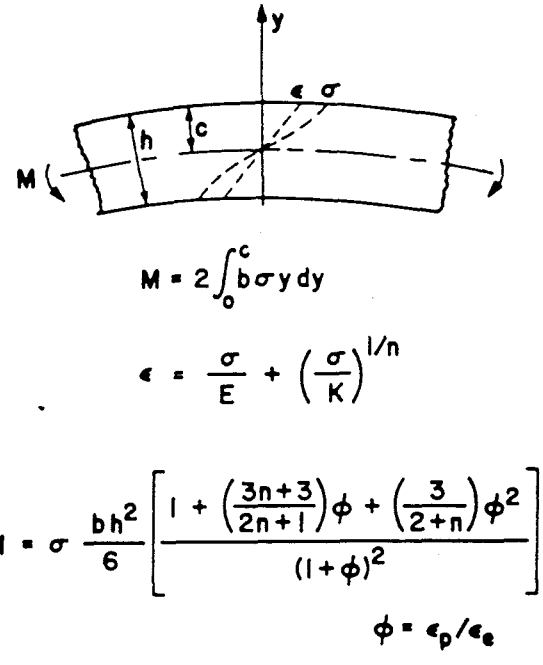


Fig. 9 - Inelastic bending analysis

This will later be used to predict decarburization effects.

PRESETTING - Presetting (bulldozing) operations are utilized to achieve dimensional uniformity and set up favorable residual stress patterns in springs. Since such processes involve relatively large deformations, it is necessary to employ bending analyses which account for inelastic material behavior. The development of an inelastic bending moment relationship is shown in Fig. 9 (8). The

analysis assumes a linear strain gradient across the section and uses a stress-gradient obtained from the stress-strain curve to determine, by appropriate integration, the resulting bending moment. Note that when $\phi=0$, i.e. behavior is elastic, the relation reduces to the familiar $M = \sigma I/c$.

This bending analysis can be used to predict the residual stresses induced as a result of presetting. The precedure is demonstrated in Fig. 10. The moment-dimension parameter is plotted as a function of surface strain using the appropriate stress-strain curves for loading and unloading. The residual strain is determined from the point of intersection of the unloading curve with the strain axis. Note that reversed plastic deformation occurs upon unloading. This residual strain information is then used, in conjunction with the material stress-strain curves, to determine the residual stresses resulting from presetting as shown in Fig. 11. Agreement between the predictions and X-ray residual stress measurements is seen to be quite good. Note that a simplified elastic unloading analysis, dashed lines, would result in substantial errors.

Another practical application of such an analysis is in the prediction of the amount of permanent set to be expected from a particular presetting operation. In Fig. 12, predictions of the amount of permanent strain associated with various prestrain levels, for the indicated hardness range of 5160 steel, is compared with experimental results. Again, agreement is very good. Also note that changes in the preexisting residual stress level resulting from presetting can be predicted from this analysis. This information, used in conjunction with specific spring geometries,

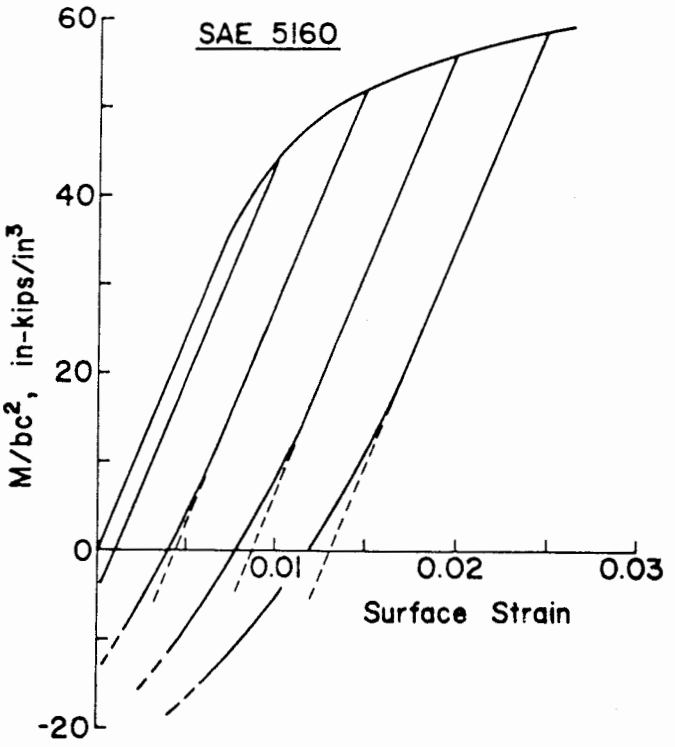


Fig. 10 - Procedure for determining residual surface strains resulting from bending prestrains

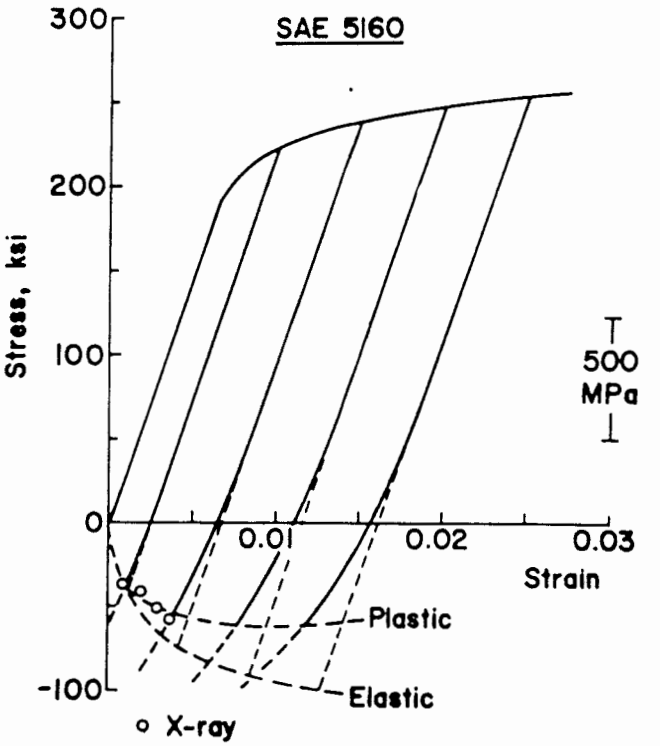


Fig. 11 - Procedure for determining residual stresses resulting from bending prestrains

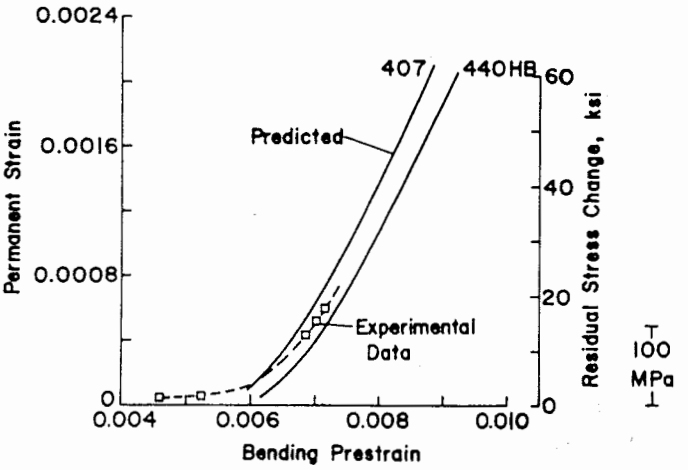


Fig. 12 - Comparison of predicted and experimental permanent strains resulting from bending prestrains

allows determination of height changes associated with various presetting operations.

SHOT PEENING/STRAIN PEENING - Residual stress profiles resulting from typical shot peening and strain peening treatments are shown in Fig. 13. Strain peening is observed to result in higher compressive stress levels and deeper penetration than conventional shot peening. Also, strain peening profiles are seen to vary with component thickness as a result of differing strain gradients during processing. Thicker sections will develop a deeper residual stress pattern, however, the maximum stress levels are little affected. The cyclic stability of such residual stress profiles will, of course, depend on the applied stress or strain level.

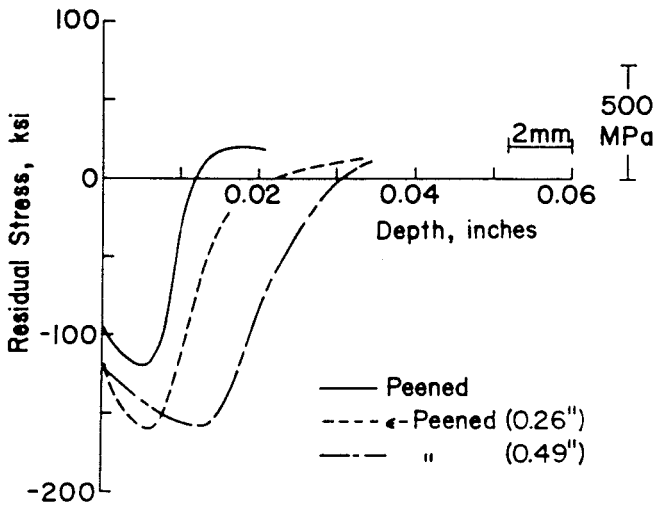


Fig. 13 - Residual stress profiles obtained with various peening operations

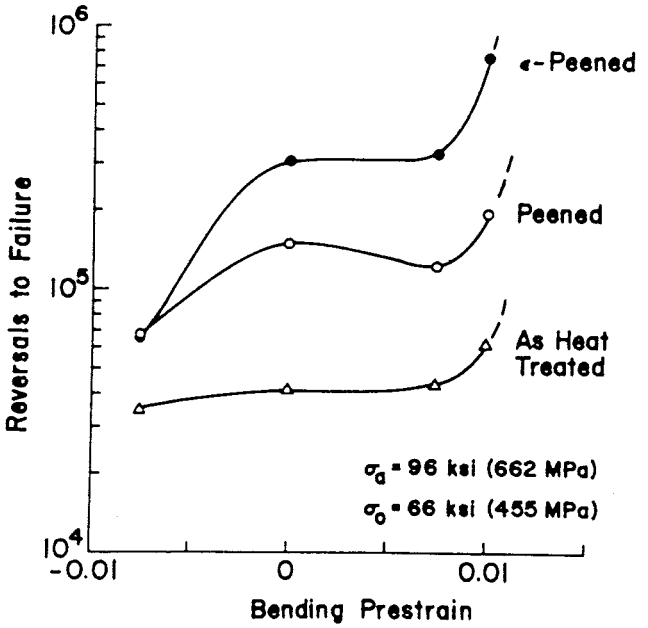


Fig. 14 - Fatigue lives of bending members subjected to various processing sequences

## FATIGUE PERFORMANCE

The results of bending fatigue tests on specimens representing a variety of processing sequences is summarized in Fig. 14. The beneficial effects of residual stresses induced by shot peening and strain peening is readily apparent. An order-of-magnitude improvement in fatigue life over the as heat treated condition is obtained by strain peening. Initial prestraining, to simulate a presetting operation, has little effect below strain levels of about 0.01. Note that reversed prestraining greatly reduces the life of peened members by reducing surface residual stress levels.

A procedure for analyzing, in detail, a surface treated bending member is shown in Fig. 15. Equation 4 is used as a damage parameter to combine information concerning material fatigue strength, $\sigma_f'$, residual stress, $\sigma_r$, applied stress amplitude, $\sigma_a$, and mean stress, $\sigma_o$. Using the stress profiles given, this parameter is plotted as a function of depth going from the surface to the neutral axis. The higher the value of the parameter, the shorter the fatigue life, thus the failure location will be indicated by the maximum in the profile. This is seen to occur below the surface where a residual tensile stress field is encountered. There is ample experimental evidence confirming that subsurface failures

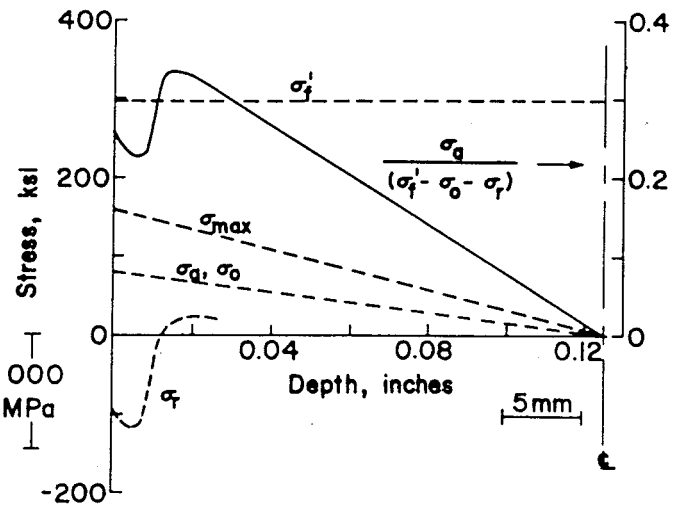


Fig. 15 - Procedure for performing fatigue analysis of a peened bending member

are common in shot peened members (2). The fatigue life can then be determined from:

$$2N_f = \left( \frac{\sigma_a}{\sigma'_f - \sigma_o - \sigma_r} \right)^{1/b} \qquad (7)$$

This analysis procedure allows determination of the influence of different processing sequences on fatigue performance.

For example, using the residual stress profiles shown in Fig. 13, damage parameter profiles are shown in Fig. 16 for bending members of two thicknesses in a peened and a strain peened condition. The deeper residual stress pattern obtained with strain peening is seen to improve fatigue life by forcing the failure site deeper. The thicker member gives shorter lives because of a more gradual applied stress gradient, i.e. the applied stresses fall off less rapidly with depth. In all instances, failure would be expected to initiate below the surface. Life predictions from this analysis compare well with the experimental results in Fig. 14. It should be noted that no attempt was made to account for stress relaxation effects in this analysis. For the stress levels used, some relaxation would be anticipated.

In Fig. 17, the influence of two levels of prestraining on residual stress and damage parameter profiles is shown. The 0.0075 prestrain level is seen to slightly diminish residual stress levels at all depths thus causing a small decrease in fatigue life. The higher prestrain level, 0.01, while decreasing compressive stresses near the surface, also deepens the residual compressive pattern thus increasing fatigue life. Note that surface and subsurface failures are about equally probable in this condition. These predicted effects are found to be generally consistent with the experimental trends in Fig. 14.

As mentioned previously, decarburization reduces material hardness near the surface which in turn alters the value of the fatigue strength coefficient, $\sigma'_f$. In Fig. 18 is shown the hardness gradient for a typical decarburized member. Using Equation 6, the variation in $\sigma'_f$ with depth can be determined. In the lower portion of the figure, damage parameter profiles are presented for members with and without decarburization. For peened members, decarburization would be expected to have little effect on fatigue performance. For strain peened members, failure is made equally probable at the surface and below the surface. These trends further suggest that the prestraining of decarburized members would degrade fatigue life by causing failure to occur at the surface.

From the foregoing, it can be concluded that the proposed analysis procedure provides reliable estimates of the effects of material, processing and geometrical factors on leaf spring performance. Thus, a useful design analysis tool is provided for optimizing spring fatigue resistance through judicious material and processing selection. Further, the

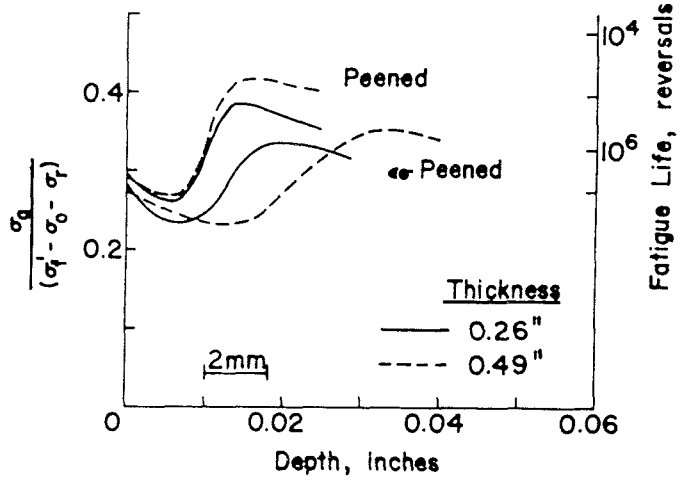


Fig. 16 - Stress parameter profiles for predicting failure location and lifetime

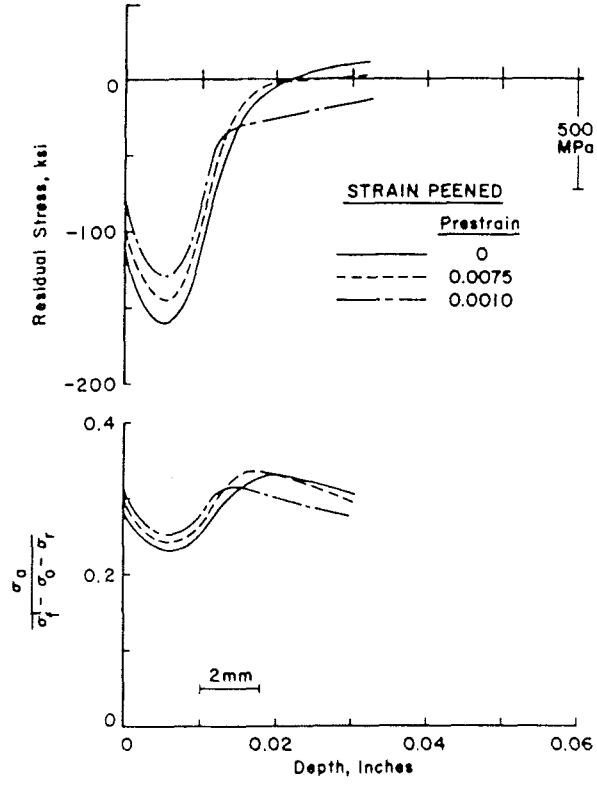


Fig. 17 - Influence of prestraining on stress profiles

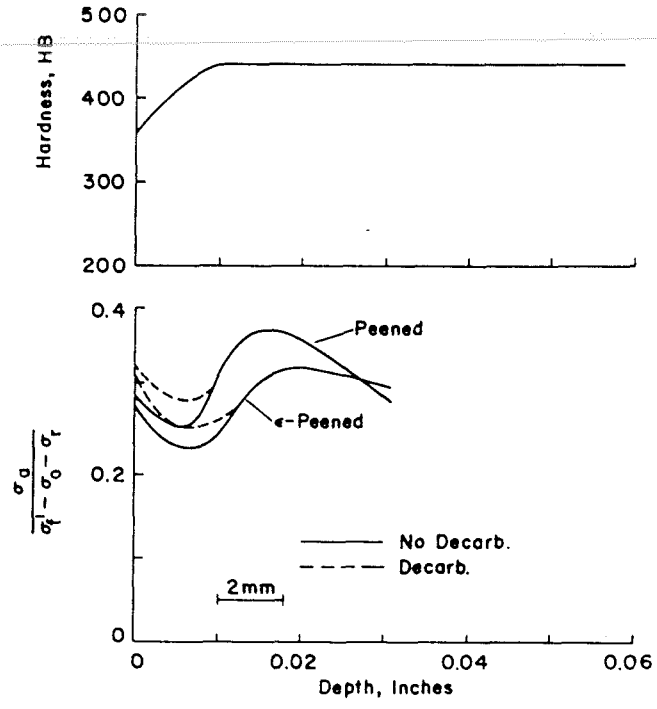


Fig. 18 - Influence of decarburization on stress profiles

approach employed is an extension of well established procedures for predicting the fatigue behavior of components in service situations. These computer-based routines are capable of modeling the various cyclic deformation responses in a structure undergoing irregular loading history, assessing damage for each event, and predicting the fatigue life. The present approach is readily adaptable to such analyses, thus further extending its usefulness in engineering design practice.

## SUMMARY

Procedures have been presented for assessing the influence of various material and processing factors on the fatigue performance of leaf springs. Cyclic deformation considerations provide a basis for determining the level and cyclic stability of residual stresses resulting from mechanical processing as well as the amount of permanent deformation associated with presetting operations. A damage parameter, incorporating material properties, residual stress effects and applied stressing conditions, provides a technique for predicting failure location and lifetime as a function of various processing sequences. Predictions obtained with this technique are in good agreement with experimental bending results.

## NOMENCLATURE

b = fatigue strength exponent
c = fatigue ductility exponent
E = elastic modulus
$\varepsilon'_f$ = fatigue ductility coefficient
$\Delta\varepsilon/2$ = strain amplitude
HB = Brinell Hardness
K = strength coefficient
$2N_f$ = number of reversals to failure
n = strain hardening exponent
r = cyclic stress relaxation exponent
$\sigma_a$ = stress amplitude
$\sigma'_f$ = fatigue strength coefficient
$\sigma_f$ = mean stress
$\sigma^o_r$ = residual stress

## ACKNOWLEDGEMENTS

The authors are indebted to Messrs. G. Grab and B. Crandall for their considerable assistance in experimental aspects of this project.

## REFERENCES

1. R. L. Mattson and W. S. Coleman, Jr., "Effect of Shot-Peening Variables and Residual Stresses on the Fatigue Life of Leaf-Spring Specimens." SAE Trans., vol. 62, 1954, p. 546.

2. R. L. Mattson and J. G. Roberts, "The Effect of Residual Stresses Induced by

Strain Peening upon Fatigue Strength." Internal Stresses and Fatigue in Metals, Elsevier Publ. Co., N.Y., 1959, p. 337.

3. R. W. Landgraf, F. D. Richards and N. R. La Pointe, "Fatigue Life Predictions for a Notched Member Under Complex Load Histories." SAE Trans., vol. 84, sect. 1, 1975, p. 249.

4. "ASTM Recommended Practice for Constant-Amplitude Low-Cycle Fatigue Testing, E606-77T." Annual Book of ASTM Standards, Part 10, Amer. Soc. Test. & Mat'ls., Phila., 1978, p. 626.

5. R. W. Landgraf, J. Morrow and T. Endo, "Determination of the Cyclic Stress-Strain Curve." Jrn. of Mat'ls., vol. 4, 1969, p.176.

6. J. Morrow, "Cyclic Plastic Strain Energy and Fatigue of Metals." Internal Friction, Damping and Cyclic Plasticity ASTM STP 378, 1965, p. 45.

7. J. Morrow, A. S. Ross and G. M. Sinclair, "Relaxation of Residual Stresses due to Fatigue Loading." SAE Trans., vol. 68, 1960, p. 40.

8. N. E. Dowling, "Stress-Strain Analysis of Cyclic Plastic Bending and Torsion." Trans. ASME, Jrn. Eng. Mater, & Tech., vol. 100, 1978, p. 157.



Society of Automotive Engineers, Inc.
400 COMMONWEALTH DRIVE, WARRENDALE, PA. 15096

12 page booklet. Printed in U.S.A.